A real-time neutron diffraction study of phase transitions in the Ti-D system after high-pressure treatment

1993 J. Phys.: Condens. Matter 5 5045

(http://iopscience.iop.org/0953-8984/5/29/003)

J. Phys.: Condens. Matter 5 (1993) 5045–5058. Printed in the UK

A real-time neutron diffraction study of phase transitions in the Ti–D system after high-pressure treatment

A I Kolesnikov†, A M Balagurov‡, I O Bashkin†, V K Fedotov†, V Yu Malyshev†, G M Mironova‡ and E G Ponyatovsky†

† Institute of Solid State Physics, Russian Academy of Sciences, 142432 Chernogolovka, Moscow District, Russia

‡ Frank Laboratory of Neutron Physics, Joint Institute for Nuclear Research, 141980 Dubna, Moscow District, Russia

Received 9 November 1992, in final form 25 February 1993

Abstract. Phase transformations in $TiD_{\sim 0.75}$ subjected to high-pressure treatment were investigated by simultaneous real-time measurements of neutron diffraction and small-angle neutron scattering. The neutron spectra were taken on heating the samples in the temperature ranges 100 to 300 K and 300 to 760 K followed by cooling to 430 K. A sequence of structural transitions was observed, which involves seven different phases and intermediate states with the hexagonal close-packed, face-centred cubic, face-centred orthorhombic or body-centred cubic metal sublattices and hydrogen atoms distributed on octahedral or ordered/disordered tetrahedral interstices.

1. Introduction

The assessed T–x diagram of the Ti–H system [1] involves a three-phase equilibrium of α, β and δ phases at the eutectoid point (figure 1)§. Here α-Ti(H) and β-TiH_x are solid solutions of hydrogen in hexagonal close-packed (HCP) α-Ti and body-centred cubic (BCC) β-Ti, and δ-TiH_{2-y} is a deficient dihydride with the face-centred cubic (FCC) metal sublattice and hydrogen atoms randomly distributed on tetrahedral interstices of the metal sublattice. A new phase has been found in near-eutectoid TiH_x samples at pressures $P \geqslant 20.5$ kbar [2, 3]. When two-phase ($\alpha + \delta$)-$TiH_{0.7-0.9}$ samples were quenched under $P \simeq 60$ kbar to 80 K and decompressed, they transformed to a single-phase state, the χ phase, which had a face-centred orthorhombic (FCO) metal sublattice [4–7]. Neutron scattering experiments [8–12] have shown that hydrogen occupied octahedral interstitials in the metal sublattice.

The χ phase was metastable at $P = 1$ atm and transformed irreversibly on heating over 95 K (115 K for deuteride) with an exothermal effect of 71 (119) J g^{-1} [13]. The main phase in the air-heated product was γ-TiH, which had an FCO metal sublattice with only 1% difference in lattice parameters a and b, but with $c/a \simeq 1.09$ [14]. Hydrogen atoms in γ-TiH were ordered on tetrahedral interstitial sites on alternate {110} planes [8–10]. The γ phase has also been observed in $TiH(D)_x$ water quenched or furnace cooled at $P = 1$ atm from about eutectoid (573 K [1]) to ambient temperature, but the content of γ-TiH in the $\alpha + \delta$ matrix of the samples did not exceed 10% [15–20].

§ Other designations were used for TiH_x phases in our previous works. They are changed herein to conform with those generally accepted now [1].

0953-8984/93/295045+14$04.50

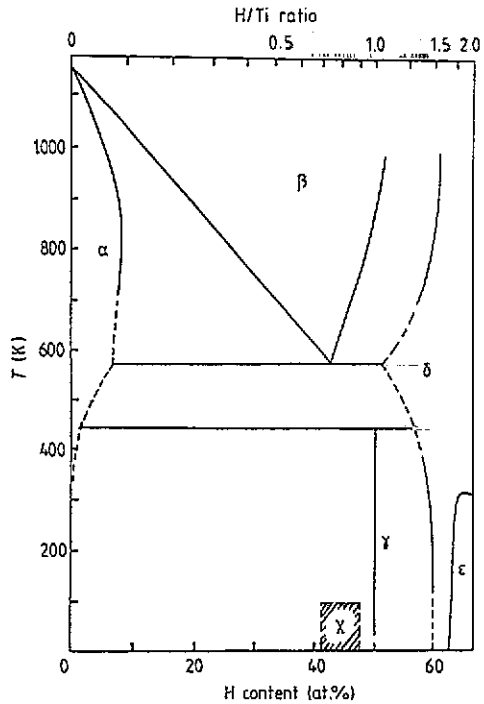

Figure 1. The T–x phase diagram of the Ti–H system [1]. Equilibrium lines near the eutectoid point are drawn after [24]. Plotted also are stability ranges for γ-TiH [12, 24]. The metastability region of the χ phase is shaded.

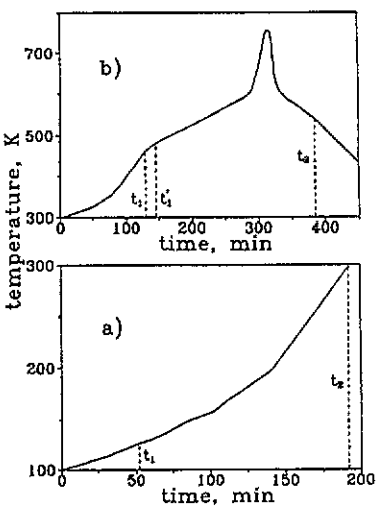

Figure 2. Sample temperature as a function of time during neutron diffraction and SANS measurements on titanium hydrides. (*a*) Low-temperature measurements; a sequence of diffraction patterns taken in the interval t_1 to t_2 is shown in figure 3. (*b*) High-temperature measurements; evolution of SANS between t_1 and t_2 is shown in figure 7, and diffraction patterns taken between t_1' and t_2 are presented in figure 8.

It was assumed from the crystal structure of γ-TiH that the γ phase was a stoichiometric monohydride, similar to γ- ZrH [21]. Therefore, excessive metal was expected to precipitate in the process of the χ to γ transformation. However, only a diffuse x-ray reflection, $d = 2.24$ Å, corresponding to (101) of α-Ti was detected after rapid heating in air [14]. This discrepancy was explained in small-angle neutron scattering (SANS) experiments on the γ-phase samples of different composition, $TiD_{0.72}$ and $TiD_{0.86}$ [22]. The SANS data led to an assumption that excessive metal precipitated during the χ to γ transformation as aggregations with the fractal dimension $D \sim 2.7$ and the crossover length $\xi \sim 85$ Å. To distinguish it from the α phase, this fine-grained titanium precipitate with highly imperfect crystal structure is denoted here as phase $\tilde{\alpha}$. On the contrary, the α-phase pattern was clearly observed in the x-ray diffraction spectra of slowly heated χ-$TiH(D)_x$ [13].

Resistivity [23] and calorimetric [13] studies of the χ to $\alpha + \gamma$ transformation have shown that this transformation was a two-stage process. An intermediate phase, κ, has been stored by means of low-temperature annealing at $\sim$ 150 K for 5 min and quenching to 77 K. Neutron diffraction and inelastic neutron scattering experiments on γ and κ phases revealed that these phases were very similar in structure and spectroscopic features in the range of energy transfer over 10 meV [10]. But a feature at $\sim$ 7 meV in the inelastic scattering spectrum of the κ phase (the same as in the χ phase) and diffuseness of superlattice

reflections led to the conclusion that this phase was a product of a partial transformation to the γ phase.

Calorimetric measurements at the $\tilde{\alpha}+\gamma$ to $\alpha+\delta$ transformation indicated thermal activity of the $(\tilde{\alpha}+\gamma)$-TiH(D)$_x$ samples over about 390 K, which preceded the endothermal peak at 441 (478) K [24]. When an $(\tilde{\alpha}+\gamma)$-TiD$_{0.70}$ sample was subjected to partial annealing treatments at several increasing temperatures, the x-ray pattern from γ-TiD did not change in the range 413 to 473 K, whereas the total x-ray pattern of the α phase appeared and increased in intensity. The decomposition reaction γ to $\alpha+\delta$ in TiD$_{0.70}$ began only at $T \simeq 473$ K [14].

There is some discrepancy in neutron diffraction data on the β phase of the Ti–H(D) system. Some authors stated that D atoms were distributed over the tetrahedral sites [16], while others [25] found the best data fit under the assumption that 15 to 30% D atoms were located in the octahedral sites. The optical vibration frequencies measured on β-TiH$_x$ by inelastic neutron scattering were consistent with hydrogen distribution on the tetrahedral sites only [26].

Thus, there was some confusion concerning both the characterization of structures of the phases involved and structural changes at phase transformations. The present real-time study of phase transformations in pressure-treated TiD$_{\sim 0.75}$ was carried out by simultaneous measurement of neutron diffraction and SANS. The total sequence of structural transformations

$$\chi \rightarrow \kappa + (\tilde{\alpha}) \rightarrow \gamma + \tilde{\alpha} \rightarrow \alpha + \delta \rightleftharpoons \beta \tag{1}$$

was investigated (only the last one is reversible), and most structures were further detailed. We parenthesize the $\tilde{\alpha}$ phase after the first transition to indicate that this phase was not a product of the transition, but arose during further evolution.

2. Experimental methods

Two samples were prepared by reaction of high-purity ($\sim$ 220 ppm) titanium with gaseous deuterium from thermally decomposed TiD$_2$ [4, 24]. The initial metal had a large grain size. To obtain fine-grained polycrystalline deuterides and to reduce their texture, the titanium rod was cold rolled by $\sim$ 70% before hydrogenation. Deuterium content was determined from weight gain, and it was $x = 0.74 \pm 0.01$ (sample I) and 0.73 ± 0.01 (sample II). Each sample consisted of 10 discs of 6.7 mm diameter and 3 mm thickness.

To produce the χ phase (Institute of Solid State Physics, Chernogolovka), the samples were compressed to 60 kbar, heated to 620 K, exposed under these conditions for 10 min, and quenched to 80 K at a rate of $\sim 10^3$ K s^{-1}. Then pressure was lowered to atmospheric [2, 7]. All further operations and storage of the χ phase were carried out under liquid nitrogen. To prepare the $\tilde{\alpha}+\gamma$ initial phase state for the high-temperature study, sample II was air-heated from the χ phase at 77 K to room temperature.

Neutron diffraction was measured using the time-of-flight diffractometer DN-2 [27, 28] at the IBR-2 reactor (Joint Institute for Nuclear Research, Dubna). The neutron scattering angles were 2ϑ = 152° and 90° for the low-temperature experiment and 160.8° and 90° for the high-temperature one. SANS was measured at the angle $2\vartheta \simeq 1°$ simultaneously with diffraction. A very high neutron flux at the sample ($\sim 10^7$ n cm^{-2} s^{-1}) and the advantage of the time-of-flight method (neutron patterns over the total Q-range are collected at each neutron impulse) ensured the temporal resolution of 0.5 min at low temperatures

and 1 min at high temperatures, which was sufficient to observe peculiarities of the phase transformations. For neutron scattering measurements in the range 100 to 300 K, sample I (the χ phase) was loaded into a cryostat with aluminium windows and then heated as shown in figure 2(a). A furnace with platinum windows was used for high-temperature measurements. Sample II (initially $\tilde{\alpha} + \gamma$) was heated from 300 to 760 K and then cooled to 430 K as shown in figure 2(b). The heating rate was lowered over 500 K in order to gain reliable statistics for Rietveld analysis. The temperature scale in the high-temperature experiment was calibrated using the onset of the eutectoid transformation on heating TiD_x as a reference point (603 K [24]). Therefore, only relative temperature variation is essential for these measurements while the absolute values of temperature are less important.

3. Low-temperature measurements

Figure 3 shows the evolution of neutron diffraction patterns from slowly heated sample I. It displays the process of $\chi \rightarrow \kappa + (\tilde{\alpha}) \rightarrow \tilde{\alpha} + \gamma$ transformations in $TiD_{0.74}$, which occurred as temperature increased from 130 to 300 K within the represented time interval (t_1 to t_2 in figure 2(a)). The spectra were observed at the angle $2\vartheta = 152°$, and they also include reflections from the aluminium walls of the cryostat. Several diffraction spectra are also represented in the left part of figure 4, as well as the corresponding SANS spectra, which are given in the right part of this figure.

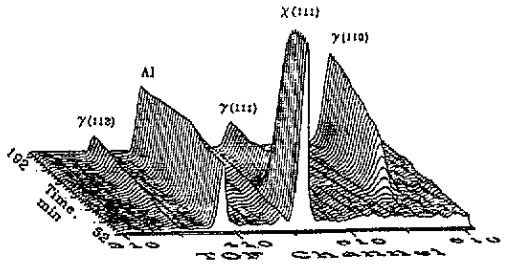

Figure 3. Evolution of the neutron diffraction pattern from $TiD_{0.74}$ (sample I) measured at the angle $2\vartheta = 152°$ during the χ to $\tilde{\alpha} + \gamma$ transformation on heating (time interval t_1 to t_2 in figure 2(a), i.e. $T = 130$ to 300 K). Numbers of the time-of-flight (TOF) channels are proportional to neutron wavelengths and interspace distances.

There were no marked changes in the diffraction spectra of the quenched phase, χ-$TiD_{0.74}$, at temperatures up to 137 K. The spectra were characterized by the only strong peak at 2.41 Å in the interval of interspace distances d = 1.5 to 3.0 Å (figure 4, at the bottom). The profile analysis of the spectrum was complicated because the sample was rather textured, in spite of the above precautions. Therefore, diffraction patterns were computer simulated for structures of orthorhombic or higher symmetry and D atoms on octahedral or tetrahedral interstices, and tested to fit the experimental spectrum. A good correlation between the calculated and experimental peak intensities was found only within the FCO structure with deuterium randomly distributed on octahedral interstices of the metal sublattice (a = 4.34 Å, b = 4.18 Å, c = 4.02 Å), which gave a strong (111) line with the structure factor $F(111) = 4|b(\mathrm{Ti}) - xb(\mathrm{D})| = 33$ fm. Here $b(\mathrm{Ti}) = -3.300$ and

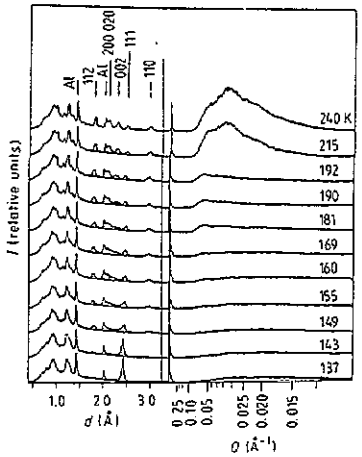

Figure 4. Representative diffraction patterns from $TiD_{0.74}$ ($2\vartheta = 152°$, left part) and SANS spectra ($2\vartheta = 1°$, right part), illustrating structural changes at the $\chi \rightarrow \tilde{\alpha} + \gamma$ phase transformation. Temperatures are given on the right, d is the interspace distance and Q is the neutron momentum transfer.

$b(D) = 6.674$ fm are coherent neutron scattering amplitudes of atoms and $x = 0.74$ is the deuterium content. The next group of intense peaks at $d = 1.22$ to 1.29 Å was indexed as {311} reflections, while the calculated intensities of {200} and {220} reflections were negligible.

The diffraction pattern drastically modified between 142 and 151 K. Peak (111) decreased in intensity by $\sim$ 5 times and shifted to larger d values (see figure 5). Simultaneously, superlattice reflections (110) and (112) arose in the pattern. These changes in the diffraction pattern can be explained by displacement of deuterium from octahedral to tetrahedral sites concomitant with ordering on alternate {110} planes and increase in volume of the unit cell. The structure factor of the (111) reflection of the formed phase, κ, is expressed as $F(111) = 4|b(Ti)| \simeq 13$ fm. Thus, the intensity ratio for (111) reflections of χ and κ phases should be equal to $I^{\chi}(111)/I^{\kappa}(111) = (F^{\chi}/F^{\kappa})^2 \simeq 6$, in good accord with the experimental value (figure 5).

Further modification of the diffraction spectrum displayed structural and chemical changes within the κ phase and its discontinuous transformation to the γ phase.

The position of peak (110) in the diffraction pattern was nearly the same between 151 and 300 K (figure 5). This indicates that lattice parameters a and b varied negligibly within the κ and γ phases. Otherwise, their variation should obey the relation $1/d^2(110) = 1/a^2 + 1/b^2 = \text{constant}$, which is less likely.

Increase in the d value for peak (111) was gradual but anomalously large between 151 and 205 K (figure 5). The relative change of $d(111)$ in this interval, $\Delta d/(d\Delta T) \simeq 10^{-4}$ K^{-1}, was much higher than linear thermal expansion of normal metal hydrides ($\sim 10^{-5}$ K^{-1} at low temperatures [29]). It is clear that such behaviour cannot be due to simple thermal expansion, but it should be attributed to increasing deuterium concentration in the κ phase. Actually, the intensity of peak (110) increased by about 1.6 times upon heating the κ phase from 151 to 205 K. According to the expression for intensity, $I(110) \sim |F(110)|^2 = |4xb(D)|^2$, this fact was evidence that the deuterium content in the κ phase increased by about 1.26 times upon its evolution, i.e. from 0.74 to 0.94.

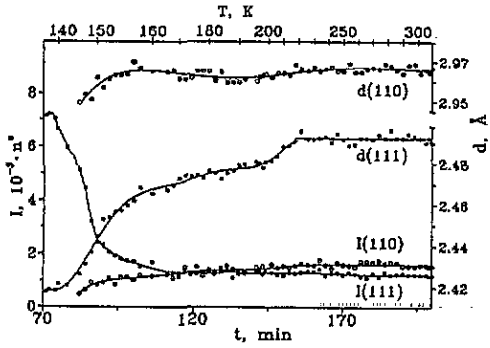

Figure 5. Temperature behaviour of intensities $I(110)$ and $I(111)$ and interspace distances $d(110)$ and $d(111)$ of the diffraction peaks in the process of $\chi \rightarrow \kappa \rightarrow \gamma$ transformation in $TiD_{0.74}$.

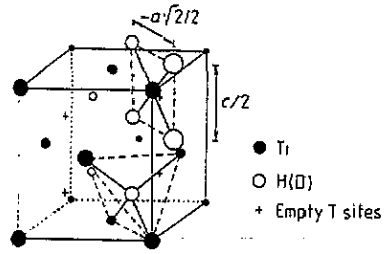

Figure 6. Positions of Ti and D atoms in the unit cell of γ-TiH(D) (FCO metal sublattice, $b/a = 1.016$, $c/a = 1.098$). Coordinates of the atoms are: Ti atoms at 0, 0, 0 and $(\frac{1}{2}, \frac{1}{2}, 0)$; H(D) atoms at $\frac{3}{4}, \frac{1}{4}, \frac{1}{4}$; $\frac{1}{4}, \frac{3}{4}, \frac{1}{4}$; $\frac{3}{4}, \frac{1}{4}, \frac{3}{4}$; and $\frac{1}{4}, \frac{3}{4}, \frac{3}{4}$. Empty interstitial sites are also shown at $\frac{1}{4}, \frac{1}{4}, \frac{1}{4}$; $\frac{3}{4}, \frac{3}{4}, \frac{1}{4}$; $\frac{1}{4}, \frac{1}{4}, \frac{3}{4}$; and $\frac{3}{4}, \frac{3}{4}, \frac{3}{4}$. Tetrahedron D–4Ti and rectangle Ti–4D are delineated with broken lines.

It is interesting to note that peak (002) overlapped with the (200) and (020) peaks below 169 K (indicated d ranges in figure 4). This range in the diffraction spectra looked like intense background between the Al (200) and κ (111) reflections rather than structural peaks. However, these peaks became well resolved on further evolution of the κ phase (190 K and higher).

A small jump in the parameter $d(111)$ occurred between 205 and 220 K, which is indicative of the κ to γ transition. Then the $d(111)$ value was nearly constant up to room temperature.

To determine structural details and the deuterium content in the γ phase as well as the occurrence of $\tilde{\alpha}$-Ti in the final product, the room-temperature neutron diffraction study was carried out with good statistics. To eliminate the effect of texture, the product was powdered to a particle size of 0.01 to 0.1 mm. The experimental data were treated under the assumption of the two-phase state of the product, i.e. $\tilde{\alpha}+\gamma$, using the multiphase profile Rietveld refinement program adapted to the time-of-flight diffractometer DN-2 [30]. Fitting of the experimental spectrum was attempted with free parameters of the $\tilde{\alpha}$ phase, but it led to unreasonable results. Therefore, lattice parameters of this phase were fixed at the values for α-Ti: $a = 2.952$ Å and $c = 4.688$ Å (space group $P6_3/mmc$) [1]. The best fit of the experimental intensities with R factors $R_W = 5.96$ and $R_P = 5.84$ was obtained for the γ phase with space group $Cccm$, deuterium occupancy $p_D = 0.96(1)$ and lattice parameters given in table 1.

It follows also from the calculated results that the content of the $\tilde{\alpha}$ phase in the final product was 19(2)%. Since the deuterium content in sample I was $x = 0.74$ and the calculated deuterium occupancy for the γ phase was $p_D = 0.96$, it is evident that the following phase relation should be observed:

$$TiD_{0.74} \rightarrow 0.23\ (\tilde{\alpha}\text{-Ti}) + 0.77\ (\gamma\text{-}TiD_{0.96}) \qquad (2)$$

i.e. the content of $\tilde{\alpha}$-Ti should be about 23%. This agrees with the calculated value within twice the error.

Table 1. Lattice parameters a, b and c, deuterium occupancies p_D, and percentage phase contents in $TiD_{0.74}$ (the top data set at 300 K where data for the $\tilde{\alpha}$ phase are taken from [1]) and in $TiD_{0.73}$ (others) at different temperatures obtained by Rietveld analysis. Numbers in parentheses are possible errors in the last digit. Space group for HCP α and $\tilde{\alpha}$ phases is $P6_3/mmc$ (No 194), for FCO γ phase $Cccm$ (No 66), for FCC δ phase $Fm3m$ (No 225) and for BCC β phase $Im3m$ (No 229).

T (K)		a (Å)	b (Å)	c (Å)	Phase content	p_D
300	$\tilde{\alpha}$	2.952		4.688	0.19	
	γ	4.168(2)	4.234(2)	4.577(1)	0.81	0.96(1)
300	$\tilde{\alpha}$	2.966(9)		4.61(2)	0.16	
	γ	4.158(1)	4.227(1)	4.571(2)	0.84	0.97(1)
380	$\tilde{\alpha}$	2.965(6)		4.63(1)	0.20	
	γ	4.164(2)	4.232(2)	4.573(2)	0.80	0.93(2)
460	$\tilde{\alpha}$	2.951(6)		4.67(1)	0.21	
	γ	4.171(2)	4.234(2)	4.567(2)	0.79	0.90(1)
520	α	2.942(3)		4.694(4)	0.54	
	γ	4.162(4)	4.251(5)	4.556(5)	0.12	0.61(3)
	δ	4.386(1)			0.34	1.53(7)
550	α	2.951(3)		4.698(3)	0.55	
	γ	4.14(3)	4.25(3)	4.54(4)	0.02	0.5(3)
	δ	4.388(1)			0.43	1.49(2)
760	β	3.3828(7)			1.00	0.73
550	α	2.946(2)		4.691(3)	0.60	
	δ	4.388(1)			0.40	1.6(3)
430	α	2.944(2)		4.682(3)	0.60	
	δ	4.388(1)			0.40	1.62(2)

The first indication of SANS was detected at $T = 180$ to 200 K in the range of neutron momentum transfer $Q = 0.05$ to 0.08 Å^{-1} (figure 4). At 200 K, SANS intensity markedly increased in the range of $Q = 0.02$ to 0.05 Å^{-1}, and then SANS spectra stabilized at 215 K.

Origination of SANS is indicative of fluctuation of neutron scattering density in the sample. It correlates with successive structural transformations concluded from diffraction data and further explains the concentration behaviour of the sample.

When the χ to κ transformation was completed, D atoms in the κ phase occupied ordered tetrahedral interstices with the occupation probability $p_D = 0.74$. Deuterium enrichment of the κ phase terminated in the formation of the stoichiometric γ phase. Both processes should result in nucleation and growth of deuterium-free regions. The neutron scattering amplitude of such regions essentially differed from the average scattering amplitude. At the first stage, nuclei of deuterium-free metal were few and small in size and could not therefore be observed in the SANS spectra. Upon evolution of the κ phase and the κ to γ transformation, these nuclei increased in number, grew in size, and combined to form regions of larger size ($\tilde{\alpha}$-Ti). Respectively, SANS drastically increased in intensity and the intensity maximum in the experimental spectra shifted to small Q values (figure 4).

The nature of κ and γ phases will be discussed now on the basis of the above data.

The anomalous temperature behaviour of lattice parameters seems to indicate strong D–D interaction in κ and γ phases. D–D distances in the χ phase are 2.9 to 3.0 Å. The D–D distance in the ab plane was nearly the same during the $\chi \rightarrow \kappa \rightarrow \gamma$ transformation, i.e. r_{ab}(D–D) = 2.97 Å in the γ phase. But that along the c axis decreased after the χ to κ transformation to r_c(D–D) = $c/2 \simeq 2.18$ Å, then gradually increased to 2.26 Å as the deuterium content in the κ phase increased (lattice parameter c calculated from the positions of (111) and (110) reflections changed from 4.365 to 4.524 Å during evolution of the κ phase).

Figure 6 shows that each deuterium atom in the γ-TiD unit cell is located in the centre of a tetrahedron of four Ti atoms. Each Ti atom also has a symmetric environment of four D atoms occupying apices of a rectangle. The κ phase has a similar unit cell, but $p_D < 1$. If we assume the central-force interaction between nearest neighbours (i.e. Ti–D) only, then increasing p_D value should lead to uniform expansion of the unit cell of the κ phase with c/a = constant (see the Ti–4D rectangle). On the contrary, the observed distortion of the unit cell results in increasing D–D distance along the c axis (the shorter side of the rectangle) while the Ti–D distance remains nearly the same as in δ-TiD_{2-y}. This indicates that the D–D interaction essentially affects the crystal structure of γ-TiD. Force constants of the D–D interaction should be much higher along the c axis than in the ab plane.

It also seems worth comparing the structural behaviour of χ-$TiD_{0.74}$ with changes in superconductivity observed by resistivity jumps in χ-$TiH_{0.71}$ in the course of successive heating runs of partial annealing [23]. It has been found that T_c of χ-$TiH_{0.71}$ decreased from 4.3 to 3.7 K after several heating runs to $T \leqslant 154$ K, then two steps at lowered T_c were observed in the resistivity curves after heating runs to $T \leqslant 165$ K; only hints of superconductivity could be fixed at $T \geqslant 1$ K after further runs, and the γ phase was non-superconductive. It can be concluded from the comparison that the κ phase is a rare case of a superconducting hydride with hydrogen partially ordered on tetrahedral sites, its T_c value being dependent on the occupancy number.

4. High-temperature measurements

Several time/temperature intervals of the spectral evolution can be distinguished on heating and cooling sample II (initially ($\tilde{\alpha} + \gamma$)-$TiD_{0.73}$). The main features of both diffraction and SANS spectra were much the same on heating to 460 K. The SANS spectrum began changing at this temperature; its evolution on heating from 460 to 760 K followed by cooling to 515 K (i.e. time interval t_1 to t_2 in figure 2(b)) is represented in figure 7. Changes in the diffraction spectra became obvious at a higher temperature of $\sim$ 480 K. The evolution of the neutron diffraction pattern taken at $2\vartheta = 160.8°$ on heating between 480 and 760 K and then on cooling to 515 K (time interval t_1' to t_2 in figure 2(b)) is shown in figure 8.

There were wide time/temperature intervals when the phase content in the sample changed rather slowly. This was used to obtain higher statistics for some temperatures by means of summing four spectra in close vicinity of the temperature. Such summary spectra were analysed using the multiphase Rietveld program†. The $\tilde{\alpha}$ phase was fitted within space group $P6_3/mmc$. Deuterium content in the $\tilde{\alpha}$ phase was accepted to be zero, $p_D = 0$, because spectrum statistics were insufficient to determine this parameter. The

† Satisfactory fits of experimental intensities were obtained here and further with R factors R_W = 5.1 to 6.4 and R_P = 5.3 to 7.7.

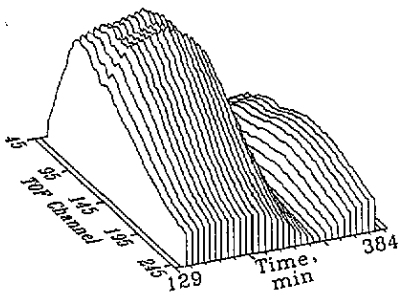

Figure 7. Evolution of the SANS spectrum ($2\vartheta = 1°$) from $TiD_{0.73}$ (sample II, initial state $\tilde{\alpha} + \gamma$) on heating between 460 and 760 K, then on cooling to 515 K (time interval t_1 to t_2 in figure 2(*b*)). TOF channel numbers are proportional to neutron wavelengths and inversely proportional to neutron momentum transfer Q. The spectra are measured simultaneously with neutron diffraction presented in figure 8.

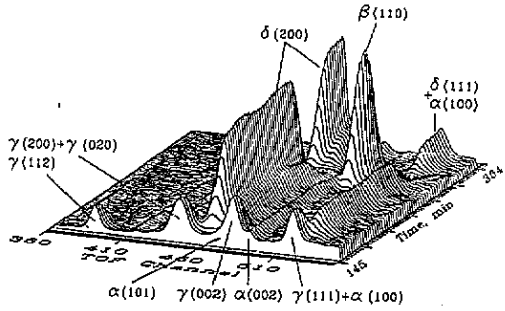

Figure 8. Evolution of the neutron diffraction pattern from $TiD_{0.73}$ measured at angle $2\vartheta = 160.8°$ on heating from 480 to 760 K followed by cooling to 515 K (time interval t_1' to t_2 in figure 2(*b*)). Representative peaks only are indicated.

results of the analysis are presented in table 1, and some diffraction patterns for different phase states are shown in figure 9.

Lattice parameters of the γ phase calculated from the room-temperature diffraction spectrum (table 1) were close to those obtained for sample I and to earlier data [12, 14, 15], but for the deuterium occupancy found by Numakura *et al* [15], $p_D = 0.85$, which seems to be too low. Parameter a calculated for the $\tilde{\alpha}$ phase was much higher while parameter c was much lower than the appropriate values reported for α-Ti(H), i.e. $a = 2.951$ and $c = 4.684$ to 4.740 Å [1].

An approximately linear increase in calculated values of lattice parameters a and b of the γ phase was observed between 300 and 460 K as could be expected due to the normal thermal expansion (figure 10). But lattice parameter c remained nearly constant. This may be due to a slight decrease of the deuterium occupancy ($p_D = 0.90$ at 460 K, table 1) relaxing the above assumed strong D–D interaction along the c axis, thus compensating thermal expansion.

The behaviour of the $\tilde{\alpha}$ phase was rather out of the ordinary in this interval. Parameter c increased while parameter a decreased linearly between 300 and 460 K (figure 11). Such behaviour was far from the normal thermal expansion, but as a result the lattice parameters of the $\tilde{\alpha}$ phase approached the values characteristic of pure α-Ti. The calculated percentage of the $\tilde{\alpha}$ phase in the sample increased from 16.4% at 300 K to 20.9% at 460 K. However, the SANS spectrum through the experimental Q-range was the same between 300 and 460 K. The invariable SANS indicates that processes at these temperatures occurred within the initial grain structure of sample II, the contrast of the $\tilde{\alpha}$-phase nuclei with respect to the average neutron scattering density being nearly the same. Otherwise, the changes took place beyond the experimental Q-range, i.e. at $Q > Q_{max} = 0.125$ Å^{-1}, which is equivalent to crystal regions of a size $l < 2\pi/Q_{max} \simeq 50$ Å. Such processes could be due to breaking of coherence between precipitated $\tilde{\alpha}$-Ti nuclei and the host γ-TiH matrix, thus formation of the normal α phase.

Phase transformation $\tilde{\alpha} + \gamma$ to $\alpha + \delta$ was evident over 480 K (figure 8). It developed rapidly to 520 K, but a small amount of the γ phase (about 1.5%) was still observed up to

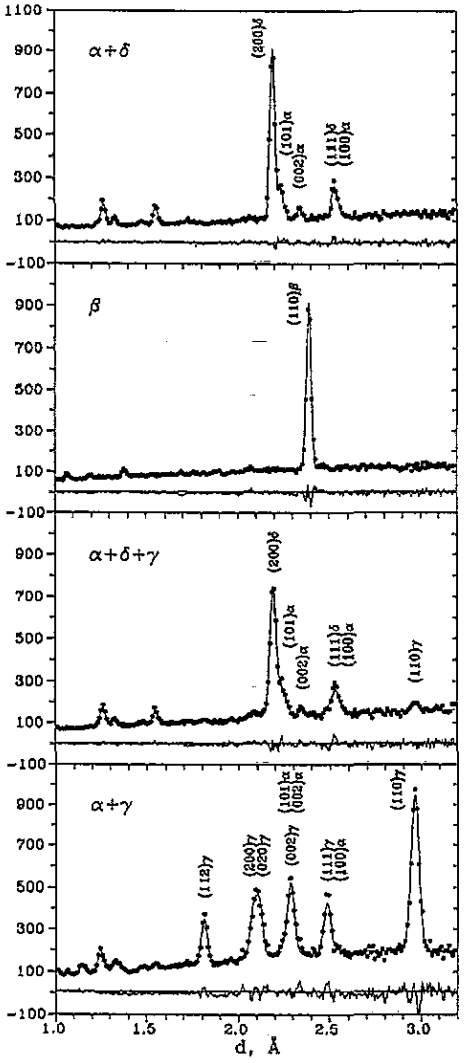

Figure 9. Rietveld refined neutron diffraction patterns characteristic of different phase states involved in the phase transformations in $TiD_{0.73}$: $\tilde{\alpha} + \gamma$ at 300 K, $\alpha + \gamma + \delta$ at 520 K, β at 760 K, and $\alpha + \delta$ at 430 K (cooled from the β phase). Shown are experimental points, fitting curves and differential curves. Some representative peaks are indicated. All patterns are plotted to the same scale.

550 K. The p_D value lowered to about 0.53 before the end of the transformation. Lattice parameters a and c decreased sharply while parameter b increased considerably during the transformation. The lattice parameter of the δ phase obtained was somewhat less than the reported value, $a = 4.397$ to 4.407 [1]. This can result from a lower value of the homogeneity limit of the δ phase at higher temperatures. The deuterium occupancy p_D at tetrahedral sites of the δ phase was 1.49 ± 0.02 at 550 K. SANS increased in intensity, and its dependence on Q markedly changed, i.e. a second maximum grew at higher channels (lower Q-values). This effect can be explained by precipitation of additional titanium owing to formation of deuterium-rich δ-$TiD_{1.49}$ from the γ phase. These titanium precipitates should

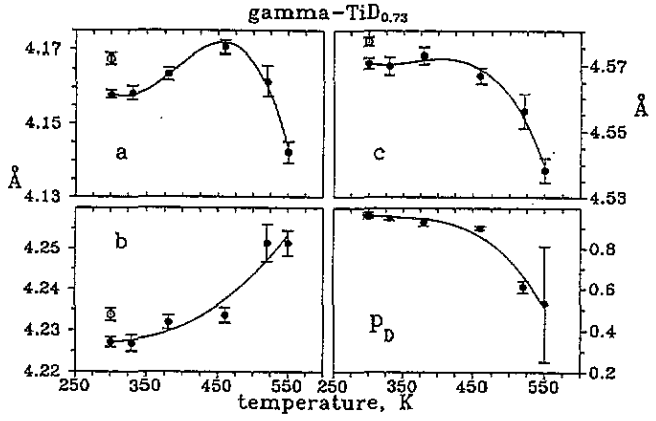

Figure 10. Lattice parameters a, b and c of the γ phase of $TiD_{0.73}$ and the deuterium occupancy p_D of the ordered tetrahedral positions in the FCO metal sublattice on heating sample II (full points). Least-squares fits with third-degree polynomials are shown as curves to visualize the temperature dependence. Open points represent data for sample I.

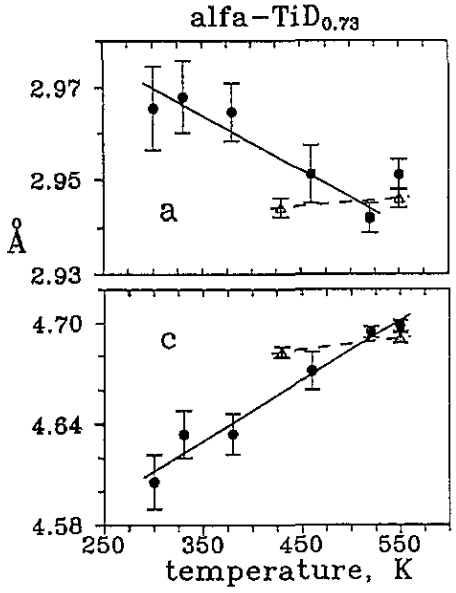

Figure 11. Lattice parameters a and c for the $\tilde{\alpha}$ phase of $TiD_{0.73}$ on heating (full circles) and for the α phase on cooling (open triangles) sample II.

be larger in size compared to Ti nuclei that precipitated upon the χ to $\tilde{\alpha}+\gamma$ transformation. By the end of the transformation, accordingly, lattice parameters in figure 11 were close to those of α-Ti.

The $\alpha+\delta$ to β phase transformation was observed at 600 to 660 K. The diffraction patterns of α and δ phases faded during the transformation in the same proportion. There were no signs of another two-phase region. It can be concluded therefore that the transformation occurred in the eutectoid point, in accordance with the earlier stated value $x_e = 0.72 \pm 0.02$ [24].

The Rietveld refinement of the neutron diffraction pattern at 760 K (figure 9) was carried out at a fixed value of the total deuterium occupancy, $p_D = 0.73$, equal to the deuterium content in the sample. Variation of the deuterium occupancies was allowed between the

tetrahedral and octahedral sites. The best fit was obtained for D atoms occupying only tetrahedral interstitial positions in the BCC metal sublattice. This result agrees with the inelastic neutron measurements [26] and neutron diffraction data [16], but disproves data [25] where 15 to 30% D atoms were assumed to be in the octahedral sites. SANS completely disappeared in the β phase, which means that the sample had no neutron scattering amplitude fluctuations, but was single phase.

On cooling, the β phase reversibly transformed to the $\alpha + \delta$ state at about the same temperatures, 660 to 590 K. The lattice parameters of the δ phase were the same as before transition to the β phase. Those of the α phase were close to the earlier reported values [1] and showed normal thermal behaviour on cooling (figure 11). The SANS intensity began growing slowly, but with some time/temperature delay compared to transformations in the diffraction spectrum. No changes were observed in the diffraction pattern below 590 K, except for normal thermal contraction, while the intensity of SANS continued to grow until 550 K. The Q dependence of SANS curves differed considerably from that on heating. The SANS intensity was much lower through the experimental range of Q, except for Q less than 0.01 Å^{-1}, where the intensity was larger than before transition to the β phase. This indicates that titanium precipitates in the $\alpha+\delta$ sample were much larger in size after cooling from the β phase than after the $\chi \rightarrow \tilde{\alpha} + \gamma \rightarrow \alpha + \delta$ transformation. This can be related to the higher temperature of the β to $\alpha + \delta$ transformation, and hence higher mobility of D atoms, whose diffusion controls growth of the products of the transformation.

A clear effect of the state and/or the grain size of precipitated titanium was also observed in the neutron diffraction patterns from sample II for different phases (figure 9). There was a marked difference between the Rietveld calculated diffraction curves for $\tilde{\alpha}$-Ti in the initial $\tilde{\alpha} + \gamma$ state at 300 K and for α-Ti in the $\alpha + \delta$ state cooled from the β phase to 430 K. The experimental data for the initial $\tilde{\alpha} + \gamma$ state could not be fitted as accurately as data for other phase states, which is evident from comparison of differential curves in figure 9. The background in the diffraction pattern from $(\tilde{\alpha} + \gamma)$-$TiD_{0.73}$ was higher, and all peaks were much broader at 300 K than in other patterns. The background gradually decreased on heating, and the peaks narrowed until the transformation to the β phase. Since the background of neutron diffraction from different crystalline phases of the same sample at some temperature is expected to be nearly the same, we believe that the observed difference in the spectra should be due to a large amount of defect and non-crystalline regions formed mainly by titanium atoms. This agrees also with the apparent increase in the percentage content of $\tilde{\alpha}$-Ti (or α-Ti) in sample II on heating and with earlier x-ray data on annealing [14].

5. Conclusions and summary

An intermediate κ phase appeared and remained over a wide temperature interval during the χ to γ phase transformation on slow heating of χ-$TiD_{0.74}$ quenched under pressure. This phase was partially ordered, i.e. deuterium occupied tetrahedral interstitial sites on alternate {110} planes of the face-centred orthorhombic metal sublattice, but the deuterium occupancy number was not stoichiometric. Deuterium content in the κ phase gradually increased until the κ to γ transformation, which was observed from the discontinuous behaviour of lattice parameter c. Precipitation of $\tilde{\alpha}$-Ti rapidly occurred at this transformation. Deuterium content in the γ phase at room temperature was close to the stoichiometric value.

The crystal structure of $\tilde{\alpha}$-Ti in $(\tilde{\alpha} + \gamma)$-$TiD_{0.73}$ prepared by rapid heating of the χ phase to room temperature differed from that of α-Ti, but gradually approached the latter

eutectoid transformation in the sample at 600 to 660 K resulted in a single-phase state, the β phase, where deuterium occupied only tetrahedral interstitial positions in the BCC metal sublattice. No SANS was observed from the β phase. The reverse transformation to the $\alpha + \delta$ state took place on cooling. Precipitated α-Ti had much larger grain size compared to $\tilde{\alpha}$-Ti and α-Ti precipitated on heating the high-pressure χ phase.

Acknowledgments

The authors thank Professor V G Glebovsky from ISSP, Russian Academy of Sciences, who supplied the high-purity titanium.

References

[1] San-Martin A and Manchester F D 1987 *Bull. Alloy Phase Diagrams* **8** 30–42, 81–2
[2] Bashkin I O, Malyshev V Yu, Rashchupkin V I and Ponyatovsky E G 1988 *Sov. Phys.–Solid State* **30** 1155–9
[3] Bashkin I O 1989 *Z. Phys. Chem. NF* **163** 469–78
[4] Ponyatovsky E G, Bashkin I O, Degtyareva V F, Rashchupkin V I, Barkalov O I and Aksenov Yu A 1985 *Sov. Phys.–Solid State* **27** 2077–8
[5] Ponyatovsky E G and Bashkin I O 1985 *Z. Phys. Chem. NF* **146** 137–57
[6] Degtyareva V F, Bashkin I O, Mogilyansky D N and Ponyatovsky E G 1986 *Sov. Phys.–Solid State* **28** 940–3
[7] Ponyatovsky E G, Bashkin I O, Degtyareva V F, Aksenov Yu A, Rashchupkin V I and Mogilyansky D N 1987 *J. Less-Common Met.* **129** 93–103
[8] Kolesnikov A I, Fedotov V K, Natkaniec I, Habrylo S, Bashkin I O and Ponyatovsky E G 1986 *JETP Lett.* **44** 509–12
[9] Kolesnikov A I, Natkaniec I, Fedotov V K, Bashkin I O, Ponyatovsky E G and Habrylo S 1989 *XI AIRAPT Int. Conf. (Kiev, 1987)* (Kiev: Naukova Dumka) pp 170–4
[10] Kolesnikov A I, Monkenbush M, Prager M, Bashkin I O, Malyshev V Yu and Ponyatovsky E G 1989 *Z. Phys. Chem. NF* **163** 709–14
[11] Kolesnikov A I, Prager M, Tomkinson J, Bashkin I O, Malyshev V Yu and Ponyatovsky E G 1991 *J. Phys.: Condens. Matter* **3** 5927–36
[12] Balagurov A M, Bashkin I O, Kolesnikov A I, Malyshev V Yu, Mironova G M, Ponyatovsky E G and Fedotov V K 1991 *Sov. Phys.–Solid State* **33** 711–14
[13] Bashkin I O, Barkalov I M, Bol'shakov A I, Malyshev V Yu and Ponyatovsky E G 1990 *Fiz. Tverd. Tela* **32** 2684–8 (in Russian) (1990 *Sov. Phys.–Solid State* **32**)
[14] Mogilyansky D N, Bashkin I O, Degtyareva V F, Malyshev V Yu and Ponyatovsky E G 1990 *Fiz. Tverd. Tela* **32** 1785–9 (in Russian) (1990 *Sov. Phys.–Solid State* **32**)
[15] Numakura H, Koiwa M, Asano H and Izumi F 1988 *Acta Metall.* **36** 2267–73
[16] Miron N F, Shcherbak V I, Bykov V N and Levdik V A 1974 *Sov. Phys.–Crystallogr.* **19** 468–70
[17] Numakura H and Koiwa M 1984 *Acta Metall.* **32** 1799–807
[18] Woo O T, Weatherly G C, Coleman C E and Gilbert R W 1985 *Acta Metall.* **33** 1897–906
[19] Bourret A, Lasalmonie A and Naka S 1986 *Scr. Metall.* **20** 861–6
[20] Numakura H, Koiwa M, Asano H, Murata H and Izumi F 1986 *Scr. Metall.* **20** 213–6
[21] Sidhu S S, Satya Murthy N S, Campos F P and Zauberis D D 1963 *Adv. Chem. Ser.* **39** 87–98
[22] Kolesnikov A I, Bashkin I O, Cotton J P, Pepy G, Ponyatovsky E G and Rosta L *8th General Conf. Condensed Matter Div. Eur. Phys. Soc. (6–9 April 1988, Budapest)*
[23] Teplinskii V M, Bashkin I O, Malyshev V Yu and Ponyatovsky E G 1989 *Fiz. Tverd. Tela* **31** 91–6 (in Russian) (1989 *Sov. Phys.–Solid State* **31**)
[24] Bashkin I O, Gurov A F, Malyshev V Yu and Ponyatovsky E G 1992 *Fiz. Tverd. Tela* **34** 1276–87 (in Russian) (1992 *Sov. Phys.–Solid State* **34** 674–80)
[25] Alperin H A, Flotow H, Rush J J and Rhyne J J 1976 *Proc. Conf. on Neutron Scattering* vol 1, ed R M Moon (Springfield, VA: National Technical Information Service, US Department of Commerce) pp 517–21
[26] Khoda-Bakhsh R and Ross D K 1982 *J. Phys. F: Met. Phys.* **12** 15–24

[26] Khoda-Bakhsh R and Ross D K 1982 *J. Phys. F: Met. Phys.* **12** 15–24

[27] Balagurov A M, Zlokazov V B, Mironova G M, Novozhilov V E, Ostrovnoii A I and Simkin V G 1989 *Communication of the Joint Institute for Nuclear Research* P3-89-601 (Dubna: JINR)

[28] Balagurov A M, Mironova G M and Simkin V G 1989 *Proc. Int. Seminar on High Temperature Superconductivity* ed V L Aksenov, N N Bogolubov and N M Plakida (Singapore: World Scientific) p 590

[29] Geld P V, Ryabov R A and Mohracheva L P 1985 *Hydrogen and Physical Properties of Metals and Alloys* (Moscow: Nauka) p 232

[30] Balagurov A M, Beskzovnyi A I, Popa N and Sangaa D 1987 *Communication of the Joint Institute for Nuclear Research* P14-87-744 (Dubna: JINR)